Campanian-Maastrichtian ocean circulation in the tropical Pacific

Claudia Jung,[1] Silke Voigt,[1] Oliver Friedrich,[1,2] Mirjam C. Koch,[1] and Martin Frank[3]

Received 24 January 2013; revised 4 July 2013; accepted 2 September 2013; published 20 September 2013.

[1] The Pacific Ocean is the largest water body on Earth, and circulation in the Pacific contributed significantly to climate evolution in the latest Cretaceous, the culmination of a period of long-term cooling. Here, we present new high-resolution late Campanian to Maastrichtian benthic and planktic foraminiferal stable isotope data and a neodymium (Nd) isotope record obtained from sedimentary ferromanganese oxide coatings of Ocean Drilling Program Hole 1210B from the tropical Pacific Ocean (Shatsky Rise). These new records resolve 13 million years in the latest Cretaceous, providing insights into changes in surface and bottom water temperatures and source regions of deep to intermediate waters covering the carbon isotope excursions of the Campanian-Maastrichtian Boundary Event (CMBE) and the Mid-Maastrichtian event (MME). Our new benthic foraminiferal $\delta^{18}O$ and Nd isotope records together with published Nd isotope data show markedly parallel trends across the studied interval over a broad range of bathyal to abyssal water depths interpreted to reflect changes in the intensity of deep-ocean circulation in the tropical Pacific. In particular, we observe a three-million-year-long period of cooler conditions in the early Maastrichtian (72.5 to 69.5 Ma) when a concomitant change toward less radiogenic seawater Nd isotope signatures probably marks a period of enhanced admixture and northward flow of deep waters with Southern Ocean provenance. We suggest this change to have been triggered by intensified formation and convection of deep waters in the high southern latitudes, a process that weakened during the MME (69.5 to 68.5 Ma). The early Maastrichtian cold interval is closely related to the negative and positive carbon isotope trends of the CMBE and MME. The millions-of-years long duration of these carbon cycle perturbations suggests a tectonic forcing of climatic cooling, possibly related to changes in ocean basin geometry and bathymetry.

Citation: Jung, C., S. Voigt, O. Friedrich, M. C. Koch, and M. Frank (2013), Campanian-Maastrichtian ocean circulation in the tropical Pacific, *Paleoceanography*, *28*, 562–573, doi:10.1002/palo.20051.

1. Introduction

[2] The climatic evolution of the Cretaceous period was characterized by the transition from a very warm mid-Cretaceous greenhouse world to a period of long-term cooling during the Late Cretaceous, culminating in the late Campanian to Maastrichtian [*Jenkyns et al*., 1994; *Huber et al*., 2002; *Forster et al*., 2007; *Friedrich et al*., 2012]. This culmination was accompanied by third-order global sea level falls [e.g., *Haq et al*., 1987; *Barrera et al*., 1997; *Li and Keller*, 1999] and several significant carbon-cycle perturbations. One of these perturbations was the so-called Campanian-Maastrichtian Boundary Event (CMBE) that is characterized by a distinct long-lasting negative carbon isotope excursion [e.g., *Barrera et al*., 1997] associated with deep and surface water cooling that regionally lagged the onset of the event by up to 600 kyr [*Friedrich et al*., 2009]. The CMBE has been recorded at different open oceanic sites in the tropical Pacific, Indian, South Atlantic, and Southern Oceans [*Barrera et al*., 1997; *Barrera and Savin*, 1999; *Frank and Arthur*, 1999; *Friedrich et al*., 2009; *Voigt et al*., 2010; *Jung et al*., 2012; *Thibault et al*., 2012a; *Voigt et al*., 2012], as well as in epicontinental seas surrounding the North Atlantic Ocean [e.g., *Odin and Lamaurelle*, 2001; *Jarvis et al*., 2002; *Jarvis et al*., 2006; *Voigt et al*., 2010; *Voigt et al*., 2012]. Slightly younger than the CMBE, the Mid-Maastrichtian event (MME) marked the termination of the early Maastrichtian cooling trend and was associated with acme occurrences of inoceramids in intermediate water depths prior to the extinction of this group of organisms during the mid-Maastrichtian [*MacLeod et al*., 1996]. The causal mechanisms of these changes in climate and the global carbon cycle are still a matter of debate, and controversial hypotheses exist. One hypothesis suggests a temporary reversal in ocean circulation manifested by the shift of intermediate to deep water sources toward high southern latitude sites [e.g., *Barrera et al*., 1997; *Li and Keller*, 1999; *D'Hondt and Arthur*, 2002; *Friedrich*

Additional supporting information may be found in the online version of this article.

[1]Institute of Geosciences, Goethe University Frankfurt, Frankfurt am Main, Germany.
[2]Institute of Earth Sciences, Heidelberg University, Heidelberg, Germany.
[3]GEOMAR Helmholtz Centre for Ocean Research Kiel, Kiel, Germany.

Corresponding author: C. Jung, Institute of Earth Sciences, Goethe University Frankfurt, Altenhöferallee 1, 60438 Frankfurt am Main, Germany. (Claudia.jung@em.uni-frankfurt.de)

0883-8305/13/10.1002/palo.20051

et al., 2009; *Koch and Friedrich*, 2012]. Another model relates observed changes in benthic foraminiferal stable oxygen isotope signatures to eustatic sea level falls [e.g., *Barrera*, 1994; *Barrera and Savin*, 1999; *Li et al*., 2000] and the buildup of small ephemeral ice sheets [e.g., *Miller et al*., 1999; *Miller et al*., 2003; *Miller et al*., 2005]. Furthermore, the exact spatial and temporal interactions of tectonic, climatic, and oceanographic processes of the latest Cretaceous are still not well constrained.

[3] In the last decades, several studies tried to reconstruct Late Cretaceous ocean circulation patterns in relation to tectonic and climatic processes by using either stable isotopes of benthic and planktic foraminifera [*Barrera*, 1994; *Frank et al*., 2005; *Friedrich et al*, 2009] or neodymium isotopes [*Frank et al*., 2005; *MacLeod et al*., 2008; *Martin et al*., 2010; *Robinson et al*., 2010; *MacLeod et al*., 2011; *Murphy and Thomas*, 2012; *Robinson and Vance*, 2012; *Voigt et al*., 2013]. Neodymium isotopes ($\varepsilon_{Nd(t)}$) are a powerful tool to reconstruct past ocean circulation patterns and their timing [*Frank et al*., 2002; *Goldstein and Hemming*, 2003]. Dissolved Nd has an oceanic residence time of between 400 and 2000 years [*Tachikawa et al*., 1999; *Frank et al*., 2002; *Arsouze et al*., 2009] similar to the global present-day oceanic mixing time (~1500 years), which allows to distinguish different water masses on the basis of their Nd isotopic composition and to use Nd isotopes as a quasi-conservative water mass tracer in the open ocean [*Goldstein and Hemming*, 2003]. In the regions of intermediate to deep water formation, water masses are labeled through weathering inputs originating from the local continental source areas. In the case of prevailing young volcanic rocks, resulting $\varepsilon_{Nd(t)}$ values are more radiogenic whereas old continental rocks are characterized by less radiogenic $\varepsilon_{Nd(t)}$ values [e.g., *Jeandel et al*., 2007]. Nd isotopes are not influenced by biological fractionation processes in seawater and thus offer the possibility to investigate changes in ocean circulation and water mass mixing on the basis of their characteristic source signatures.

[4] The Nd isotope signature of marine deep waters is recorded in archives such as fish debris and ferromanganese oxide coatings of sediment particles formed through early diagenetic processes at the sediment water interface and is additionally affected by differential leaching of volcanic ash inputs and exchange processes with sediment particles described as boundary exchange [*Lacan and Jeandel*, 2005; *Horikawa et al*., 2011; *Le Houedec et al*., 2012]. In the present study, we used ferromanganese oxide coatings of bulk sediments as an archive to reconstruct the deep water Nd isotope composition of Campanian-Maastrichtian sediments in the tropical Pacific. Only a few studies used this approach thus far for Cretaceous sediments [e.g., *Voigt et al*., 2013], while earlier work commonly applied Nd isotope compositions of fossil fish debris [*Thomas*, 2004; *Frank et al*., 2005; *Pucéat et al*., 2005; *MacLeod et al*., 2008; *Robinson et al*., 2010; *MacLeod et al*., 2011; *Jiménez Berrocoso et al*., 2012; *Martin et al*., 2012; *Robinson and Vance*, 2012]. Recently, it has been proposed that both archives, sediment coatings and fish debris, deliver indistinguishable results for Cretaceous sediments [*Martin et al*., 2010; *Martin et al*., 2012].

[5] Although the resolution in most of the Cretaceous studies is not very high, some general trends and patterns are observed so far. Studies from the Tethys [*Pucéat et al*., 2005; *Soudry et al*., 2006] showed a change of NW Tethyan $\varepsilon_{Nd(t)}$ values from less radiogenic values during the Santonian to Early Campanian toward more radiogenic values until the Maastrichtian. This has been interpreted to reflect a change in deep water source regions from a high-latitude North Atlantic source to a source in the North Pacific or Southern Ocean, possibly activated by a strong westward flowing circumglobal Tethyan current located at the southern Tethyan margin [*Pucéat et al*., 2005; *Soudry et al*., 2006]. In the Southern Ocean, *Robinson et al.* [2010] and *Robinson and Vance* [2012] interpreted the shift toward less radiogenic Nd isotope signatures during the early Campanian as a consequence of the sinking of Southern Component Water (SCW) triggered by long-term climatic cooling and opening of tectonic gateways. The formation and advection of SCW was proposed to have acted as the major mechanism of deep-ocean ventilation during the late Campanian to Maastrichtian sourcing deep waters in the North Atlantic via the Central Atlantic Gateway, as well as in the proto-Indian Ocean [*Robinson and Vance*, 2012]. *MacLeod et al.* [2008] and *Jiménez Berrocoso et al.* [2010] found very low $\varepsilon_{Nd(t)}$ values during Cenomanian to Maastrichtian times at Demerara Rise (tropical North Atlantic), which has been referred to as Demerara Bottom Water. This locally formed water mass, labeled with the unradiogenic signature of the Guyana shield, is supposed to have been replaced by a water mass formed in the North Atlantic that had driven global ocean circulation since the late Maastrichtian [*MacLeod et al*., 2011]. *Murphy and Thomas* [2012], instead, concluded from neodymium isotope data obtained from sites in the proto-Indian and the tropical Pacific that deep water formation in the Indian Ocean was only regionally important because of paleogeographic and bathymetric barriers. This interpretation is in contrast to the other studies before, which all assume a mode of globally overturning circulation for the Late Cretaceous oceans. However, the argument by *Murphy and Thomas* [2012] was recently strengthened by results of *Voigt et al*. [2013], who proposed that Walvis Ridge has acted as a barrier that prevented deep water exchange between the Atlantic and the Southern Ocean until the late Maastrichtian based on unusually radiogenic Nd isotope signatures on the ridge crest of Walvis Ridge. These authors supposed that tectonic restriction promoted a mode of ocean circulation in the Atlantic and Southern Ocean mainly driven by numerous regionally formed intermediate and deep water sources.

[6] The Pacific Ocean, instead, occupied a much greater proportion of the global ocean during the Cretaceous and early Cenozoic than today and thus also had a larger influence on global oceanic heat transport [*Kamenkovich et al*., 2000] and global climate than the other ocean basins. Available benthic oxygen isotope and neodymium isotope data from the Pacific Ocean are interpreted to indicate shifts between different deep and intermediate-water sources during the early to middle Maastrichtian, inferred to represent different sources of deep water production in the Southern Ocean and the North Pacific [*Thomas*, 2004; *Frank et al*., 2005; *Hague et al*., 2012]. The temporal resolution of these studies, however, is relatively low and does not allow for a detailed consideration of Nd isotope shifts relative to the carbon-cycle perturbations of the CMBE and MME.

[7] To improve the current data base and to achieve a better understanding of Late Cretaceous oceanic circulation and its

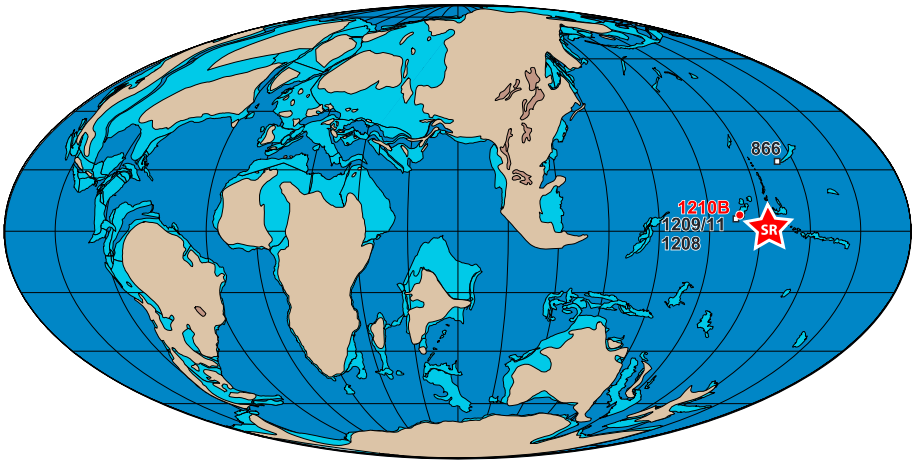

Figure 1. Paleogeographic reconstruction of the late Campanian (70 Ma; [*Hay et al*., 1999]), showing the location of ODP Hole 1210B on Shatsky Rise (filled circle). Other sites in the Pacific Ocean are highlighted by squares. SR, Shatsky Rise.

driving factors, we here present new high-resolution benthic and planktic foraminiferal stable isotope records combined with Nd isotope data obtained from ferromanganese oxide coatings of bulk sediment from Ocean Drilling Program (ODP) Hole 1210B at Shatsky Rise in the tropical Pacific Ocean. Hole 1210B is located in the open tropical Pacific where local weathering contributions from the surrounding continents are negligible for the deep water Nd isotope compositions. Using these proxy records, we reconstruct the evolution of tropical Pacific surface and deep water temperatures and changes in ocean circulation and environmental conditions during the Campanian to Maastrichtian time interval at high temporal resolution and compare these results with previous publications [e.g., *Frank et al*., 2005] (Figure 2 and Figure S1 in supporting information). Our new data are less noisy and resolve temporal trends in relation to the CMBE and MME carbon isotope excursions in unprecedented detail compared with previously published Nd and stable isotope data. The very high resolution of our 13 Myr record provides the first detailed reconstruction of short-term changes in ocean circulation in the tropical Pacific during the latest Cretaceous (~79 to 66 Myr).

2. Geological Setting

2.1. Hole 1210B

[8] Hole 1210B (ODP Leg 198) was drilled on the southern flank of the Southern High of Shatsky Rise (western central Pacific; 32°13.4203′N, 158°15.5623′E; Figure 1) in a water depth of 2573 m. The paleowater depth is assumed to have been similar or somewhat shallower [*Kaiho*, 1999]. Shatsky Rise is the oldest existing oceanic plateau, which is located ~1600 km east of Japan and was formed in Late Jurassic to Early Cretaceous times [~147 to 135 Ma; *Nakanishi et al*., 1989]. During the Maastrichtian, the Shatsky Rise was situated at a paleolatitude of ~10°N [*Larson et al*., 1992].

[9] The studied sedimentary of Hole 1210B (cores 24-1 to 40-2) belong to Lithologic Unit III and range from the lower Campanian to the uppermost Maastrichtian (66.18 to 78.92 Ma; 218.85–351.25 m below seafloor (bsf)) [*Bralower et al*., 2002a]. Unit III consists of white nannofossil ooze, nannofossil ooze with foraminifers, and chert layers. The unlithified ooze intervals have carbonate contents of 96–100 wt % [*Bralower et al*., 2002a]. Based on high-resolution carbon isotope stratigraphy, the sedimentation rate was estimated to be ~1.3 cm/kyr during the Campanian and Maastrichtian [*Jung et al*., 2012]. Biozonation is based on planktic foraminifera [*Bralower et al*., 2002b] and calcareous nannofossils [*Lees and Bown*, 2005]. Sections 198-1210B-28-4 and 28-6 (260.73–264.12 m bsf) document a short interval with abundant shell debris of inoceramids [*Bralower et al*., 2002b], which is considered to represent ocean-wide changes in circulation [*MacLeod et al*., 1996].

2.2. Age Model

[10] Time control for ODP Hole 1210B is based on the age model of *Voigt et al*. [2012] which provides a global correlation of Late Cretaceous high-resolution carbon isotope records between shelf-sea and oceanic sites. The $\delta^{13}C$ record of Gubbio (Italy) serves as a reference curve using an age of 72.1 Ma for the Campanian-Maastrichtian boundary. The $\delta^{13}C$ correlation established by *Voigt et al*. [2012] allows the detection of distinct carbon isotope events (Late Campanian Event, Campanian-Maastrichtian Boundary event (CMBE), mid-Maastrichtian event (MME), Cretaceous-Paleogene Boundary Event (K/Pg)) which can be also correlated to the bulk-carbonate $\delta^{13}C$ record of Hole 1210B [*Jung et al*., 2012]. These events have been related to the geomagnetic polarity scale recalculated using the astronomical $^{40}Ar/^{39}Ar$ calibration of the Fish Canyon sanidine [*Kuiper et al*., 2008]. Correlation between Gubbio and Shatsky Rise is based on the comparison of their similar $\delta^{13}C$ evolutions and is supported by the relative timing of base occurrences of stratigraphic index fossils [*Bralower et al*., 2002b; *Lees and Bown*, 2005; *Petrizzo et al*., 2011]. An age of 72.8 Ma was assigned to the beginning of the CMBE [*Voigt et al*., 2012].

3. Material and Methods

3.1. Stable Carbon and Oxygen Isotopes

[11] A total of 548 samples from 218.85–351.25 m bsf of ODP Hole 1210B were analyzed for foraminiferal stable isotopic compositions. Samples were dried, weighed, and washed over a 63 µm sieve. From the dried samples, an

average of 30 individuals of the planktic foraminiferal species *Rugoglobigerina rugosa* was picked from the 150–212 µm fraction using a standard binocular microscope. For samples with less than 30 individuals, the entire size range was picked. A total of 510 samples were analyzed for planktic foraminiferal stable isotopes from core sections 25 to 40 at a resolution of 20 cm corresponding to approximately 15 kyr based on the sedimentation rate of 1.3 cm/kyr [*Jung et al*., 2012]. For benthic foraminiferal stable isotopes, the epifaunal species *Nuttallides truempyi* was picked from the 150–500 µm fraction. Due to the partly sporadic occurrence of this species, a total of 301 samples (typically 20 to 80 cm resolution corresponding to 15 to 60 kyr) have been analyzed for benthic foraminiferal stable isotopes across the studied succession. Stable carbon and oxygen isotope compositions were measured with a Finnigan MAT 253 mass spectrometer equipped with a Gasbench II (Goethe University Frankfurt, Germany). Isotopic ratios are expressed in per mil (‰) deviations from the Vienna Peedee Belemnite standard. The analytical precision of replicates of standard measurements was better than 0.02 and 0.06‰ for carbon and oxygen, isotopes, respectively.

3.2. Nd Isotopes

[12] Neodymium was extracted from early diagenetic Fe-Mn oxide coatings on bulk sediment samples following the method described by *Gutjahr et al*. [2007]. Approximately 6 g of the dry bulk sediment of 48 samples from Hole 1210B were rinsed three times with de-ionized water (from a Milli-Q system, MQ). Samples were mixed with 20 mL of a 15% acetic acid/Na acetate buffer solution several times and put in a shaker overnight until the carbonate was completely removed. After that, the samples were rinsed three times with de-ionized water. The decarbonated samples were leached with a 0.05 *M* hydroxylamine hydrochloride (HH)/15%-acetic acid solution (in a 1:1 mixture of MQ:HH), buffered to a pH of 3.6 with NaOH, to reduce and dissolve the oxide coatings. Recent evidence for changes in the extracted Nd isotope ratio as a function of changes in sample to solution ratios [*Piotrowski et al*., 2012; *Wilson et al*., 2013] are not an issue for our sediments given the excellent correspondence to fish teeth data of some of the very same samples (see below). The supernatant was pipetted after centrifugation for further chemical treatment. The detrital fraction was then rinsed three times with de-ionized water and dried afterward. Finally, ~50 mg of dried bulk sediment were dissolved in a mixture of concentrated HF and HNO_3 to determine the isotopic composition of the detrital material. The supernatant for isotopic analysis was dried down and redissolved in 0.5 mL 1 *M* HCl prior to column chemistry.

[13] Leachates and dissolved detrital fractions were passed through three sets of ion exchange columns following published standard procedures for Sr [*Horwitz et al*., 1992; *Bayon et al*., 2002] and Nd [*Cohen et al*., 1988; *Barrat et al*., 1996; *Le Fèvre and Pin*, 2005]. $^{87}Sr/^{86}Sr$ ratios from some leached coatings and detritus samples were measured to evaluate the seawater origin of the Nd isotope data. Firstly, Sr and the rare earth elements were separated using a cation exchange column. A second column used 50 µL Sr Spec resin to separate Sr from Rb. The third column used Ln-Spec resin to collect Nd and elute Ba and the other rare earth elements (REEs). Nd isotopes were analyzed on a Nu Plasma Multicollector-Inductively Coupled Plasma-Mass Spectrometer at GEOMAR, Helmholtz Centre for Ocean Research Kiel, Germany. The samples were diluted with 2% HNO_3 to achieve a ~18 V total beam for Nd using a DSN-100 nebulizer. All measured $^{143}Nd/^{144}Nd$ ratios were mass fractionation corrected to $^{146}Nd/^{144}Nd = 0.7219$ and then normalized to the accepted ratio for the international JNdi-1 neodymium isotopic standard of 0.512115 [*Tanaka et al*., 2000], which was analyzed after every sixth sample. During the measurements for this study, the JNdi-1 standard showed an external long-term reproducibility of ±0.000011 (2σ), which corresponds to ±0.3 ε_{Nd} units (2σ). Procedural Nd blanks were ≤25 pg [*Stumpf et al*., 2010]. The Nd isotope composition ($^{143}Nd/^{144}Nd$) is expressed in the $\varepsilon_{Nd(0)}$ notation which corresponds to $[(^{143}Nd/^{144}Nd)_{sample}/(^{143}Nd/^{144}Nd)_{CHUR} - 1] \times 10^4$, where CHUR = 0.512638 (CHUR = Chondritic Uniform Reservoir, which represents the present-day average earth value) [*Jacobsen and Wasserburg*, 1980].

[14] The measured Nd isotope values were decay corrected to the time of deposition to calculate $\varepsilon_{Nd(t)}$. Therefore, an average $^{147}Sm/^{144}Nd$ ratio of 0.124 was determined by using the available ratios from the authigenic ferromanganese oxide coatings on bulk sediment samples from the Cretaceous Site 1210. This correction for measured $^{143}Nd/^{144}Nd$ ratios is represented by $\varepsilon_{Nd(t)} = [(^{143}Nd/^{144}Nd)_{sample(t)}/(^{143}Nd/^{144}Nd)_{CHUR(t)} - 1] \times 10^4$ [*DePaolo and Wasserburg*, 1976]. $^{143}Nd/^{144}Nd_{CHUR(t)}$ was calculated using $^{147}Sm/^{144}Nd_{CHUR(today)} = 0.1967$. Measured $^{87}Sr/^{86}Sr$ ratios were corrected for instrumental mass bias using $^{88}Sr/^{86}Sr = 8.3752$ and were normalized to the accepted value for National Institute of Standards and Technology SRM987 of 0.710245. The 2σ external reproducibility of repeated standard measurements was always better than 35 ppm.

4. Results

4.1. Carbon and Oxygen Isotopes

4.1.1. Carbon Isotopes

[15] The planktic foraminiferal carbon isotope ($\delta^{13}C_{pl}$) record shows pronounced variability on shorter time scales, in particular during the Maastrichtian (Figures 2 and S1). In the late Campanian (79.0 to 75.5 Ma) $\delta^{13}C_{pl}$ compositions are essentially constant with values around 2.5 to 2.6‰ followed by a rise to 3.1‰ between 75.5 and 74.5 Ma, which appears more abruptly in the bulk-carbonate record. Above this interval, the $\delta^{13}C_{pl}$ record shows distinct negative excursions between 74.5 and 73.7 Ma and at 70.7 Ma with rather stable values and superimposed short-term variations in between. This intermittent horizon comprises the CMBE interval (72.8 to 70.5 Ma) according to global carbon isotope correlations [*Jung et al*., 2012; *Voigt et al*., 2012]. Interestingly, the distinct negative carbon isotope excursion, which characterizes the initial CMBE elsewhere, is not recorded in the $\delta^{13}C_{pl}$ signal at Hole 1210B. In the early Maastrichtian, between 70.7 and 69.0 Ma, the $\delta^{13}C_{pl}$ values display a distinct rise toward a maximum of 3.4‰ immediately before the MME. This carbon isotope increase is a prominent feature of the global carbon cycle recorded in many sections worldwide and also in the bulk-carbonate $\delta^{13}C$ record at Hole 1210B [*Jung et al*., 2012]. The MME itself is characterized in the $\delta^{13}C_{pl}$ record by a brief negative inflection at 69.0 Ma that occurs

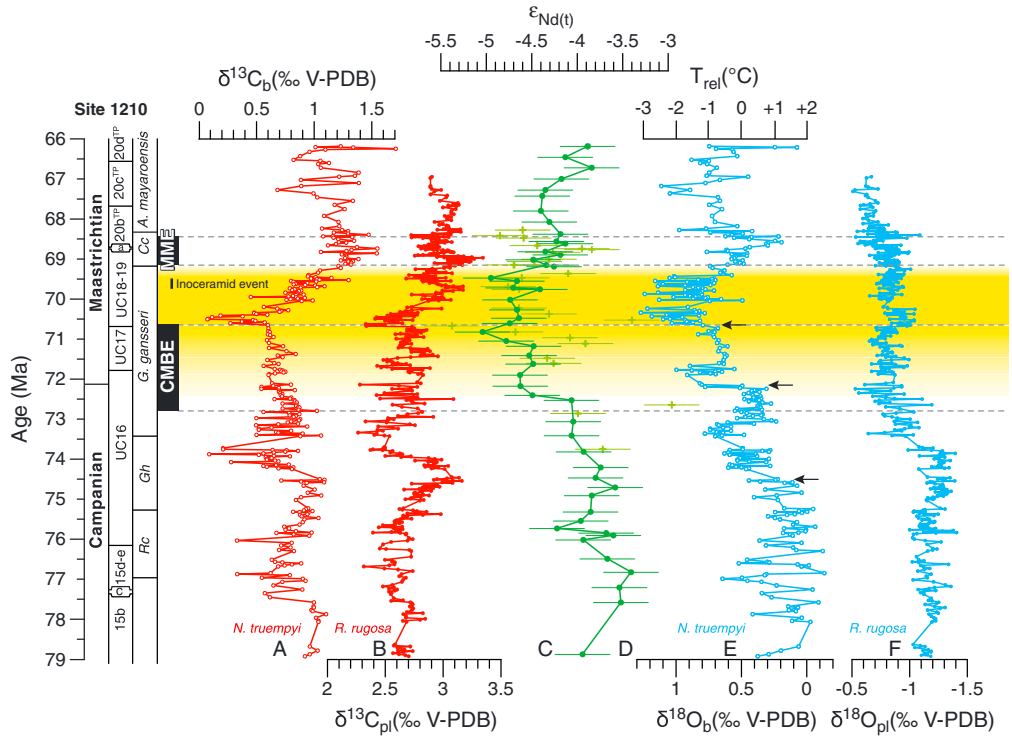

Figure 2. Compilation of planktic (filled circles) and benthic (open circles) foraminiferal $\delta^{13}C$ (A and B) and $\delta^{18}O$ (E and F) data together with bottom water Nd isotopes signature obtained from ferromanganese oxide coatings (green circles; C, error bars denote 2σ external reproducibilities) and fish debris (green crosses; D; [*Frank et al.*, 2005]) from Site 1210, Shatsky Rise. The age model is based on a biostratigraphically calibrated carbon-isotope correlation [*Voigt et al.*, 2012] using the Fish Canyon sanidine calibration [*Kuiper et al.*, 2008]. The yellow bar marks a period of bottom water cooling and enhanced admixture of waters with Southern Ocean provenance. Arrows highlight periods of concomitant shifts in $\delta^{18}O_b$ (see text). Abbreviations: CMBE, Campanian-Maastrichtian Boundary Event; MME, mid-Maastrichtian event; c, 15c; a, 20a.

superimposed on a long-term global maximum. After 67.6 Ma, $\delta^{13}C_{pl}$ values tend to decrease, a trend that continued until the end of the Maastrichtian as also recorded in the bulk-carbonate $\delta^{13}C$ data.

[16] The long-term trend of the benthic foraminiferal carbon isotope ($\delta^{13}C_b$) record is similar to that of planktic foraminifera, although the amplitude of variations is larger and therefore more distinctive (Figures 2 and S1). The $\delta^{13}C_b$ record shows values of ~1‰ between 78.9 and 77.5 Ma and then decreases abruptly by ~0.4‰ at 77.4 Ma from where it increases again back to values around 1‰ between 77.4 and 74.5 Ma (Figure S1). Similar to the planktic $\delta^{13}C$ record, $\delta^{13}C_b$ values show two prominent negative excursions of nearly 1‰ between 74.35 and 73.7 Ma and at 70.5 Ma. These minima bracket the CMBE, which itself is characterized by slightly decreasing $\delta^{13}C_b$ values until 70.5 Ma. After the second negative post-CMBE $\delta^{13}C_b$ excursion, $\delta^{13}C_b$ values display a 1‰ rise toward the MME (68.8 Ma) where maximum values of 1.5‰ are reached. Above the MME, the $\delta^{13}C_b$ record shows relatively constant values between 1 and 1.5‰ apart from a shift to higher values toward the end of the Maastrichtian (66.3 Ma).

4.1.2. Oxygen Isotopes

[17] Planktic foraminiferal oxygen isotope data ($\delta^{18}O_{pl}$) show only small variations during the studied time interval. The record starts with constant values of ~−1.2‰ until 73.7 Ma (Figures 2 and S1) and a subsequent increase of ~0.5‰ in the latest Campanian (from −1.3‰ to about −0.8‰ between 73.7 and 72.9 Ma). This transition occurs during the first broad negative carbon isotope excursion before the CMBE. During and after the CMBE, the signal

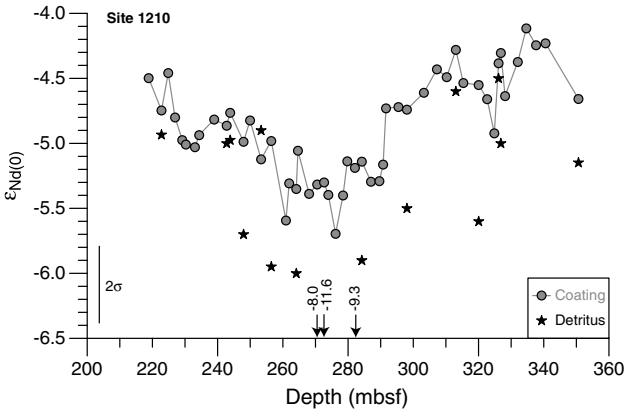

Figure 3. Late Cretaceous $\varepsilon_{Nd(0)}$ composition from ferromanganese oxide coatings (circles) and sediment detritus (stars) for Site 1210. Three $\varepsilon_{Nd(0)}$ data from detritus samples plot outside the given Nd isotope range. The error bar denotes 2σ external reproducibility.

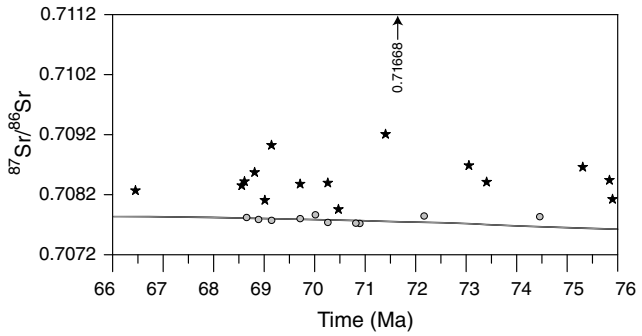

Figure 4. Plot of $^{87}Sr/^{86}Sr$ ratios of coatings (circles) and dissolved detritus (stars) relative to the seawater strontium isotope curve (grey line; *McArthur et al*., 2012). The error bars (2σ) are smaller than the size of symbols.

is almost stable (~−0.8‰) until the end of the MME (68.65 Ma). The pattern of the $\delta^{18}O_{pl}$ curve differs from that observed in the bulk-carbonate $\delta^{18}O$ record [*Jung et al*., 2012], which displays an ongoing trend of rising values in the course of the CMBE between 72.9 and 70.0 Ma (Figure S1). After the MME (~68.0 Ma), the $\delta^{18}O_{pl}$ values show a small increase to values of up to −0.5‰.

[18] The long-term trend of the benthic oxygen isotope ($\delta^{18}O_b$) record differs distinctly from the $\delta^{18}O_{pl}$ record. Benthic foraminiferal oxygen isotope data were relatively constant between 79.0 and 74.5 Ma displaying a broad minimum between 75.0 and 78.0 Ma (Figure S1). Thereafter, the $\delta^{18}O_b$ values show a long-term rise with superimposed discrete steps of rising values at 74.5, ~72.0, and 70.5 Ma (arrows in Figure 2). Before and during the earliest CMBE (73.2–72.2 Ma), the long-term rise of $\delta^{18}O_b$ values is interrupted by a short decrease. After the CMBE between 70.5 and 70.2 Ma, the $\delta^{18}O_b$ record reaches highest values of 1.2‰. The onset of this interval corresponds to the second negative carbon isotope excursion that terminated the CMBE. From 70.2 Ma onward until the MME (68.5 Ma), the $\delta^{18}O_b$ values show a distinct decrease reaching a minimum during the MME (68.5 Ma). This decrease corresponds to the early Maastrichtian $\delta^{13}C$ rise (Figure S1). After the MME, the $\delta^{18}O_b$ record increases again until 67.2 Ma and subsequently decreases toward the K/Pg boundary.

4.2. Neodymium Isotope Results

[19] Variations of the $\varepsilon_{Nd(t)}$ values at Hole 1210B show a striking similarity to the variations of the $\delta^{18}O_b$ record (Figure 2). The Nd isotope signatures obtained from the ferromanganese oxide coatings range from −3.4 to −5.1 (Figure 2). Between 78.9 and 74.5 Ma, $\varepsilon_{Nd(t)}$ signatures are almost constant with values of -3.8 ± 0.3, although they display a broad inflection between 75.0 and 78.0 Ma similar to the $\delta^{18}O_b$ values. From 74.5 Ma until 72.5 Ma, $\varepsilon_{Nd(t)}$ values decrease slightly up to −4.1. The interval around 72.5 Ma is marked by a sharp decrease of $\varepsilon_{Nd(t)}$ toward a period of less radiogenic Nd isotope signatures, which prevailed during the CMBE and in the early Maastrichtian until 69.5 Ma. The three-million-year-long period of relatively unradiogenic $\varepsilon_{Nd(t)}$ values (up to −5.1) coincides with the interval of maximum $\delta^{18}O_b$ values. After 69.5 Ma, a shift to more radiogenic $\varepsilon_{Nd(t)}$ values reaches its maximum of −4.1 during the MME and is followed by more stable signatures. A further increase of Nd isotopes occurs at the end of the Maastrichtian (67.0 Ma) when the benthic $\delta^{18}O$ record shows decreasing values, and the $\varepsilon_{Nd(t)}$ record almost reaches initial signatures of the late Campanian. Our new results agree with previously published Nd isotope data derived from fish debris [*Frank et al*., 2005], and with few exceptions both records plot within error of each other (Figures 2 and S1). Our new Nd isotope record, however, has the advantage of being less noisy and having a higher temporal resolution allowing the detection of trends in relation to the CMBE and MME carbon isotope excursions in unprecedented detail.

[20] Neodymium isotope compositions of the detrital fraction as well as strontium isotope compositions of both ferromanganese oxide coatings and the detrital fraction from Site 1210 have been measured to estimate the accuracy and reliability of Nd isotope data obtained from the coatings as an archive of past seawater composition (Figures 3 and 4). Especially during the Campanian-Maastrichtian transition, the detrital fraction of the sediments shows less radiogenic $\varepsilon_{Nd(0)}$ values between −9.3 and −5.7 than the coatings (Figure 3). But for some samples, Nd isotope ratios of detritus and leached coatings are identical and exhibit more radiogenic values between −5.7 and −4.5. This partial similarity of $\varepsilon_{Nd(t)}$ values of detritus and leached coatings is either coincidental given that the major Pacific deep water mass also has similar signatures or may have been either caused by partial dissolution of the detrital fraction during leaching of the coatings or from early diagenetic remobilization of REEs from volcanic rocks [*Martin et al*., 2010]. In order to constrain detrital contamination of the leached seawater Nd isotope signatures, strontium isotope ratios on leached coatings and the detritus were measured (Figure 4). The $^{87}Sr/^{86}Sr$ signatures of the detritus samples range between 0.70796 and 0.71668 and are distinctly more radiogenic than the coeval seawater strontium isotope curve (Figure 4). The $^{87}Sr/^{86}Sr$ signatures of leached coatings, in contrast, follow the seawater strontium isotope curve with only a small deviation toward more radiogenic values [*McArthur et al*., 2012]. Although a minor contribution of detritus leaching cannot be completely excluded, the good agreement of strontium isotope ratios with the seawater signal also argues for a seawater origin of the Nd isotopes in the analyzed coatings. As demonstrated by *Gutjahr et al*. [2007], small deviations of the Sr isotope signature of the coatings are mostly still consistent with reliable bottom water Nd isotope signatures given that the amount of Sr in the detrital fraction is much higher than that of Nd and therefore a slight dissolution of the detrital fraction will already change the Sr isotope signature of the leachate but leave its Nd isotope signature unaffected. The main argument for the reliability of the data is the excellent agreement of the Nd isotope signatures derived from sediment coatings and fish debris [*Frank et al*., 2005], which confirm the results of *Martin et al*. [2010, 2012] that both archives deliver indistinguishable results. Consequently, $\varepsilon_{Nd(t)}$ values of leached coatings at Site 1210 are considered to reliably represent past seawater signatures.

5. Discussion

5.1. Foraminiferal Preservation

[21] Benthic and planktic foraminifera of Hole 1210B are generally moderately well to well preserved with little fragmentation

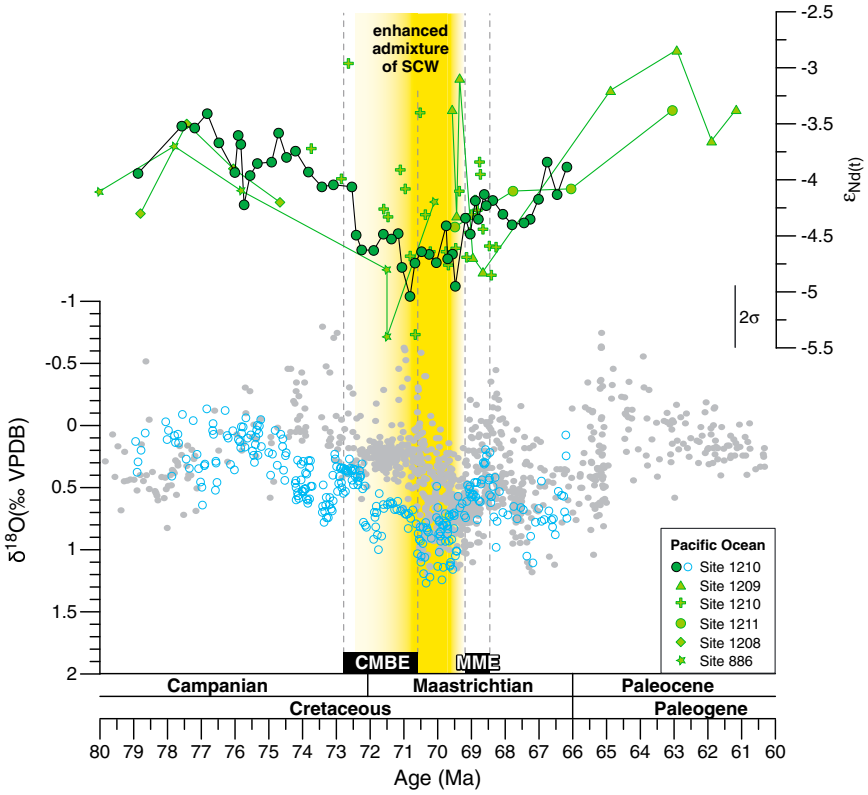

Figure 5. Comparison of the new $\varepsilon_{Nd(t)}$ and $\delta^{18}O_b$ records of Site 1210 with previously published Late Cretaceous to early Paleogene neodymium isotope data from various water depths in the Pacific Ocean and the global benthic foraminiferal oxygen compilation rescaled to the GTS12 timescale (grey circles; *Zachos et al*. [2001]; *Friedrich et al*. [2012]). Data are from the following sites and present-day water depths: Site 1210, 2573 m (dark green and open blue circles, this study; green crosses, *Frank et al*. [2005]); Sites 1209 and 1211, 2387 and 2907 m (green triangles and circles, *Thomas* [2004]); Site 886, 5713 m (green stars, *MacLeod et al*. [2008]); and Site 1208, 3346 m (green diamonds, *Murphy and Thomas* [2012]). The vertical bar denotes 2σ external reproducibility. The period of enhanced admixture of Southern Component Water (SCW) in the Pacific Ocean is highlighted by the colored bar. Abbreviations: CMBE, Campanian-Maastrichtian Boundary Event; MME, mid-Maastrichtian event.

observable under a standard binocular microscope. Under a scanning electron microscope, however, the wall structures of the planktic foraminifera show signs of recrystallization and minor secondary sparite growth. Since such an early diagenetic recrystallization takes place after settling on the seafloor, $\delta^{18}O_{pl}$ values have possibly been altered toward cooler temperatures [*Paull et al*., 1988]. The clear and consistent gradient between benthic and planktic foraminiferal $\delta^{18}O$ values in our records, however, suggests that most of the original signal is still preserved, although the calculation of absolute sea surface temperatures (SST) is hampered. Therefore, we only consider relative changes in SST inferred from $\delta^{18}O_{pl}$ rather than absolute paleotemperatures.

[22] The benthic foraminiferal signal is not so much altered, because benthic foraminifera are less recrystallized and/or the alteration took place under early diagenetic conditions when temperatures were the same as the deep water mass. Further support comes from the fact that $\delta^{18}O_b$ and $\delta^{13}C_b$ values from Hole 1210B show a long-term trend that is within the range of the global compilation of benthic foraminiferal stable isotope data [*Friedrich et al*., 2012] (see Figure 5 for $\delta^{18}O$) that are considered to be essentially unaltered by diagenesis [e.g., *Barrera*, 1994; *Barrera et al*., 1997; *Li and Keller*, 1998; *Friedrich et al*., 2009].

5.2. Carbon Isotope Signatures

[23] The carbon isotope record derived from bulk carbonates at Hole 1210B [*Jung et al*., 2012] shows distinct variations in its long- and short-term trends which allow a detailed correlation to other $\delta^{13}C$ records worldwide, in particular to the $\delta^{13}C$ record of the Gubbio section [*Voigt et al*., 2012] which serves as stratigraphic reference for paleomagnetic and microfossil zonation [e.g., *Arthur and Fischer*, 1977; *Premoli Silva and Sliter*, 1995; *Gardin et al*., 2012]. Based on this correlation, the CMBE and MME intervals can be precisely placed at Hole 1210B, although both features are less distinctly developed at Shatsky Rise than elsewhere. The new planktic $\delta^{13}C$ record ($\delta^{13}C_{pl}$) of this study closely resembles variations recorded in the bulk-carbonate $\delta^{13}C$ record in both magnitude and absolute value but also shows some peculiarities (Figure S1).

[24] At Shatsky Rise, the CMBE is represented by a minor long-lasting negative $\delta^{13}C_b$ decrease bracketed by two prominent negative excursions (Figures 2 and S1). Regional

carbon isotope correlation among different sites at Shatsky Rise shows the lower negative excursions to be represented by a hiatus at greater water depth (Site 305) reflecting periods of erosion as a result of mass wasting and/or changes in the strength of bottom currents [*Jung et al*., 2012]. Both processes can result in an alteration of the carbon isotope signal by increased oxidation of organic matter and/or increased diagenetic cementation of chalk. The lower $\delta^{13}C_b$ excursion shown in our records of Site 1210 is interpreted as a regional feature that is not related to changes in the global carbon cycle.

[25] After the CMBE, our data show a pronounced positive trend of both the $\delta^{13}C_b$ and $\delta^{13}C_{pl}$ records reaching maximum values during the MME. This $\delta^{13}C$ maximum has been observed in numerous studies from different oceanic and shelf settings, such as the Lägerdorf-Kronsmoor-Hemmoor [*Voigt et al*., 2010] and Stevns-1 core [*Thibault et al*., 2012b] records from the European chalk sea, sites 690 and 525 in the Southern Ocean [*Barrera et al*., 1997; *Friedrich et al*., 2009], and Hole 1210B in the tropical Pacific [*Frank et al*., 2005; *Jung et al*., 2012]. For Hole 1210B, previously published $\delta^{13}C_b$ and $\delta^{13}C_{pl}$ data [*Frank et al*., 2005] show the same trend as our new data but with a significantly lower resolution (Figure S1). The similarity of the Shatsky Rise $\delta^{13}C$ records during the CMBE and MME to carbon isotope records elsewhere strongly supports the reliability of our new data set, which is interpreted to reflect a major perturbation of the global carbon cycle rather than being caused by local changes in productivity or circulation.

[26] The CMBE covers a time span of 2.3–2.5 Myr with the initial negative $\delta^{13}C$ excursion lasting ~1 Myr (72.8–71.8 Ma) [*Voigt et al*., 2012]. This time span is too long to explain the carbon-cycle change solely by glacioeustasy as supposed by *Barrera and Savin* [1999], *Li et al*. [2000], *Miller et al*. [2003], and *Miller et al*. [2005]. The long duration of the CMBE together with a rather slow initiation is more indicative for large-scale earth processes such as changes in plate-tectonic configuration [*Müller et al*., 2008a], mid-ocean ridge subduction [*Müller et al*., 2008b], or hot spot volcanism [*Frey et al*., 2000; *Coffin et al*., 2002] as triggering mechanisms. These tectonic processes might have caused changes in oceanic bathymetry and shelf-sea size and/or in the exchange of deep waters between oceanic basins and thus could have influenced the magnitude of the ^{12}C transfer into reduced (i.e., organic-carbon-rich) sedimentary reservoirs.

[27] *Voigt et al*. [2012] suggested a relation between depositional environment and the magnitude of the CMBE $\delta^{13}C$ excursions, which is larger in shelf seas and in the narrow ocean basins of the Atlantic and Southern Ocean compared to the open oceanic environment of the Pacific. The reasons for the higher sensitivity of smaller carbon reservoirs are complex and might be related in some degree to diagenetic effects but also to a more effective carbon partitioning of dissolved inorganic carbon in smaller water bodies (see discussion in *Voigt et al*. [2012]). Recent evidence from neodymium isotope records from the South Atlantic and Southern Ocean support the idea of a limited global exchange of deeper water masses in Late Cretaceous times [*Voigt et al*., 2013]. This implies that oceanic carbon reservoirs were smaller and therefore more affected by regional organic-carbon sources and sinks probably leading to the differences in the magnitude of the CMBE excursion observed in different settings.

5.3. Pacific Ocean Circulation During the Campanian-Maastrichtian

5.3.1. Late Campanian to CMBE (79.0 to 74.5 Ma)

[28] Benthic foraminiferal oxygen isotope data provide information about variations in both deep-sea temperatures and continental ice volume, while carbon isotope data recorded changes in the global carbon cycle as well as ventilation of deep waters [e.g., *Zachos et al*., 2001]. Concomitant variations in $\delta^{18}O_b$ and $\delta^{13}C_b$ during the latest Cretaceous have been discussed as a consequence of relatively large and geologically rapid changes of the marine and atmospheric carbon content which may have directly contributed to the long-term global climatic cooling [*D'Hondt and Lindinger*, 1994]. These fluctuations of the $\delta^{18}O$ and $\delta^{13}C$ records have been reported from all major ocean basins (the North Atlantic [e.g., *Barrera and Savin*, 1999; *Friedrich et al*., 2004], the South Atlantic [*e.g*., *Barrera and Savin*, 1999; *Li and Keller*, 1999; *Friedrich et al*., 2009], the Indian Ocean [e.g., *Barrera*, 1994; *Barrera and Savin*, 1999], and the tropical Pacific [e.g., *Barrera et al*., 1997; *Barrera and Savin*, 1999; *Li and Keller*, 1999]), indicating changes in surface and bottom water temperatures and ocean circulation that characterized the Campanian to Maastrichtian time interval.

[29] The early Campanian (83.0 to 78.0 Ma) was a time of climate cooling which supposedly triggered the formation of Southern Component Water around Antarctica [*Thomas et al*., 2003; *Robinson and Vance*, 2012]. Between 78.0 and 74.5 Ma (late Campanian), $\delta^{18}O_b$ values suggest a time of general global warming followed by another cooling trend until the end of the Cretaceous [*Friedrich et al*., 2012] (Figure 5).

[30] At Hole 1210B, the late Campanian period is characterized by invariant Nd isotope signatures of bottom waters as well as uniform $\delta^{18}O$ records of planktic and benthic foraminifera indicating stable surface and bottom water temperatures (79.0 to ~74.5 Ma; Figure 2). This interval was terminated by a ~2°C cooling starting at ~74.5 Ma affecting both surface and bottom waters. The onset of bottom water cooling, however, led surface water cooling by ~1 Ma and occurred well before the CMBE carbon isotope perturbation, a feature which has not been observed in other proxy records before. Some previously published benthic and planktic oxygen isotope data at Hole 1210B are of lower resolution and do not dissolve the long-term trend (Figure S1) [*Frank et al*., 2005]. While the absolute values of $\delta^{18}O_{pl}$ plot in the same range as in our record, it has to be noted that the $\delta^{18}O_b$ data of *Frank et al*. [2005] are distinctly lower with much more scatter compared to our record.

[31] Late Campanian $\varepsilon_{Nd(t)}$ bottom water values at Hole 1210B (~2573 m water depth) show a radiogenic composition (~−3.8) between ~78.9 and 74.5 Ma, followed by a small shift to less radiogenic values (~ −4.1) until 72.5 Ma, which coincide with bottom water cooling as indicated by increasing $\delta^{18}O_b$ values before the CMBE. This first weak shift to less radiogenic values in our record coincides with the beginning of the second global cooling phase of the latest Campanian from 74.5 Ma onward [*Friedrich et al*., 2012] also recorded at other locations in the Southern Ocean and the tropical Pacific [*Frank et al*., 2005; *MacLeod et al*., 2008; *Murphy and Thomas*, 2012]. Tropical Pacific Nd

isotope data along a depth transect at Shatsky Rise (ODP Sites 1209 (located at 2387 m present-day water depth; *Thomas* [2004]), 1208 (3346 m; *Murphy and Thomas* [2012]), 1211 (2907 m; *Thomas* [2004]), and 1210 [*Frank et al*., 2005]), although of lower resolution than our record, broadly follow the trend recorded for Hole 1210B (Figure 5). ODP Site 886 located at the Chinook Trough toward NE in ~3021 km distance from Shatsky Rise (Figure 1) represents abyssal water depths (5713 m) and is thus deeper than the other sites [*MacLeod et al*., 2008]. The Nd isotope signatures at Site 886 are slightly less radiogenic than those at Shatsky Rise but display a very similar long-term trend. All records in the Pacific Ocean therefore show essentially the same trends and values, suggesting that a large range of water depths (~2300 to 5700 m today) in the Late Cretaceous Pacific was affected by the same water mass. From 74.5 Ma onward, a common shift to less radiogenic values occurred (Figure 5). This uniform change of Nd isotopic signatures in the late Campanian thus reflects a lack of stratification and an overall change in deep-ocean circulation.

[32] Radiogenic Nd isotope values of bottom waters in the modern tropical Pacific are the consequence of tectonically and climatically driven weathering and drainage of young circum-Pacific volcanic arc system [*Goldstein and Jacobsen*, 1987; *Horikawa et al*., 2011] caused by the subduction of the Kula and Farallon Plates, a process that has been active since the mid-Cretaceous (~110 Myr) [*Larson and Pitman*, 1972]. Sources for radiogenic values in the modern Pacific mainly comprise volcanic rock of the Kourile Islands, as well as island arcs and subduction zones along the western and eastern Pacific margins and the Antarctic Peninsula. Furthermore, radiogenic values are released by islands resulting from intraplate volcanism, such as Tahiti and Hawaii [*Jeandel et al*., 2007]. The various Nd isotope values in the modern Pacific Ocean show that different parts of the Pacific are influenced differently by local sources [*Horikawa et al*., 2011]. *Horikawa et al*. [2011] demonstrated that a less radiogenic deep water mass (~−8 ε_{Nd}) from the Southern Ocean flows into the North Atlantic. In contrast, the central equatorial Pacific and western equatorial Pacific exhibit values of −3.5 to −3.1 ε_{Nd}. This significant alteration of seawater ε_{Nd} values from south to north is mainly caused by mixing of waters from the Southern Ocean with more radiogenic North Pacific waters. Introduction of the radiogenic Nd isotope signatures in the North Pacific and partly the central Pacific Ocean occurs through partial dissolution of particles, such as in the eastern equatorial Pacific [*Grasse et al*., 2012], as well as exchange of ambient bottom water Nd signatures with sediment and rock particles (boundary exchange) [*Lacan and Jeandel*, 2005] and reversible scavenging [*Siddall et al*., 2008] and/or by a combination of all [*Arsouze et al*., 2009; *Horikawa et al*., 2011]. Seawater neodymium isotope signatures in the modern Pacific are as radiogenic as the $\varepsilon_{Nd(t)}$ values during the latest Cretaceous. This suggests that boundary exchange and reversible scavenging might have changed the seawater ε_{Nd} values of northward flowing SCW the equatorial Pacific in a similar way as today. The late Campanian (79 to 74.5 Ma) ε_{Nd} trend toward less radiogenic neodymium isotopes at Shatsky Rise thus likely represents enhanced admixture of cooler SCW into the equatorial Pacific region during the generally cooler climate conditions. *Frank et al*. [2005] supposed that changes in the Pacific neodymium isotope signatures are related to variable contributions of different water masses with different provenance (SCW versus North Pacific deep waters). Based on the uniform Nd isotope trends we observed at Shatsky Rise and Site 886 at different water depths, we suggest that a single, uniform water mass affected ocean circulation in the Late Cretaceous Pacific but with variable strengths of deep water formation at the source region (Southern Ocean) and subsequent admixture into the Pacific. This model infers that no deep water formation occurred in the North Pacific Ocean or that a potential North Pacific deep water source was too weak to influence the tropical Pacific Ocean.

5.3.2. CMBE to Late Maastrichtian (74.5 to 66.0 Ma)

[33] The $\delta^{18}O_{pl}$ record across the CMBE at Hole 1210B does not show a pronounced positive oxygen isotope trend. Such an absent cooling in the earliest Maastrichtian has not been observed in other studies yet. Elsewhere, $\delta^{18}O_{pl}$ values show a positive trend across the CMBE that is generally less pronounced than in $\delta^{18}O_b$ [e.g., *Barrera and Savin*, 1999; *Li and Keller*, 1999; *Friedrich et al*., 2009] (Figures 2 and S1). Our new data suggest that tropical Pacific SSTs were largely unaffected by the CMBE in contrast to other ocean basins.

[34] The benthic foraminiferal oxygen isotope data of Hole 1210B indicate a gradual displacement of the prevailing warmer waters by more intense admixture of cooler SCW between 74.5 and 69.5 Myr. Most pronounced cooling occurred in a three-million-year-long period (72.5–69.5 Ma) with maximum bottom water cooling (~3 °C) at around 70.5 Ma (Figure 2). This early Maastrichtian cool period is coeval to a shift of about one $\varepsilon_{Nd(t)}$ unit toward less radiogenic neodymium isotope signatures (−4 to −5), which is also indicated in other tropical Pacific records, although of lower resolution (Sites 886, 1208, 1209, 1210, and 1211) [*Thomas*, 2004; *MacLeod et al*., 2008; *Murphy and Thomas*, 2012] (Figure 5). The concomitant appearance of a cooler and less radiogenic water mass at multiple sites refers to a lack of stratification in the deeper water column and an overall change in deep-ocean circulation during early Maastrichtian times. We suggest this change to represent variations in the strength of northward deep water flow related to increased production of cooler and well-oxygenated intermediate to deep waters in the Southern Ocean. Cool SCW acquired its less radiogenic signature by weathering of different old continental and less radiogenic source regions such as the Australian margin, the Prydz Bay sector of the Antarctic terranes [*Roy et al*., 2007], or the Exmouth Plateau. Despite increased advection, mean $\varepsilon_{Nd(t)}$ values of Pacific bottom waters (−4.5 to −5.0) did not reach the contemporaneous unradiogenic end-member values of the Southern Ocean sites (~−10) [e.g., *Robinson et al*., 2010; *Murphy and Thomas*, 2012] (Figure 5). This suggests that, as today, SCW became increasingly diluted by mixing with northern and central Pacific water masses and was also modified by boundary exchange, particle dissolution, and reversible scavenging during its northward flow into the Pacific Ocean.

[35] Between ~69.5 and 68.5 Ma, benthic $\delta^{18}O_b$ values decreased significantly, reflecting a ~4°C warming of bottom waters during the MME. Simultaneously, $\varepsilon_{Nd(t)}$ values increased to more radiogenic values (−4.1 to −4.5) (Figure 2) and together with the lower $\delta^{18}O_b$ values suggest a return to a late Campanian mode of circulation, when global intermediate and/or deep water production in the Southern Ocean was

less strong during a period of significant global warming [*Friedrich et al*., 2012].

5.4. Wider Implications

[36] Overall, our new data show that deep waters originating in the Southern Ocean had a substantially greater influence on the Central Pacific during periods of climate cooling than compared to warming periods, a process obviously linked to higher rates of deep water production in the Southern Ocean [e.g., *Friedrich et al*., 2009; *Robinson and Vance*, 2012]. The observed changes in tropical Pacific intermediate to deep waters imply a widespread and synchronous change in global deep-ocean circulation as inferred by the parallel cooling trend documented by the global compilation of $\delta^{18}O_b$ [*Friedrich et al*., 2012] (Figure 5).

[37] Our new Shatsky Rise record documents a systematic change from warm late Campanian bottom waters to enhanced admixture of cooler water masses with Southern Ocean provenance during the early Maastrichtian. This change occurred simultaneously with significant global cooling as reflected by benthic foraminiferal oxygen isotopes [*Friedrich et al*., 2012]. Coolest bottom water temperatures occurred in the time interval between the CMBE and MME carbon isotope excursions and are not related to supposed periods of sea level fall, arguing against a significant ice cover on Antarctica. Overall global warming during the late Maastrichtian on the other hand commenced with the MME and was accompanied by a change of ε_{Nd} values and $\delta^{18}O_b$ data in the opposite direction, suggesting a return to the previous state with a weaker formation of SCW. These conditions still prevailed across the transition from the Cretaceous to the Cenozoic as documented by Pacific $\varepsilon_{N(t)}$ records [*Thomas*, 2004] (Figure 5). The observed synchronicity of global climate change and changes in bottom water circulation in the tropical Pacific shows that climatic warming and cooling periods were the main drivers of the intensity of SCW formation and therefore circulation changes during the latest Cretaceous. The beginning and termination of the early Maastrichtian cooling and intensified deep-ocean circulation in the Pacific fall into the periods of the initial negative CMBE-$\delta^{13}C$ excursion and the subsequent $\delta^{13}C$ rise toward the MME, respectively, suggesting a linkage to the causes of long-term carbon-cycle perturbation. The close relation of the early Maastrichtian cool period to the negative and positive carbon isotope trends of the CMBE and MME together with its millions-of-years-long duration argues for tectonic forcing of climatic cooling. Tectonic processes as hot spot volcanism or mid-ocean ridge subduction may have caused changes in oceanic bathymetry and/or in the exchange of deep waters between oceanic basins, which influenced deep oceanic convection and the intensity of ocean circulation in the Pacific Ocean.

6. Conclusions

[38] Gaining information about the role of the Pacific Ocean is an important prerequisite to understand global ocean circulation during the Late Cretaceous. High-resolution stable carbon and oxygen isotope analyses of benthic and planktic foraminifera and neodymium isotope compositions of bottom waters reconstructed from ferromanganese oxide coatings from the Campanian/Maastrichtian tropical Pacific Ocean indicate major changes in surface and deep water temperatures and in the relative contribution of deep waters with Southern Ocean provenance. Our new data allow the following conclusions:

[39] 1. Between 79.0 and 74.5 Ma, foraminiferal $\delta^{18}O$ values indicate relatively warm bottom and sea surface temperatures in the tropical Pacific. At the same time, Nd isotope signatures indicate pronounced radiogenic Nd input from volcanic sources through boundary exchange and reversible scavenging.

[40] 2. All sites at Shatsky Rise and in the North Pacific display uniform Nd isotope signatures over a wide range of water depths inferring the presence of a single, nonstratified intermediate to deep water mass in the Late Cretaceous Pacific Ocean.

[41] 3. Surface and bottom water oxygen isotope signatures reveal a cooling prior to the CMBE with the onset of bottom water cooling leading surface water cooling by ~1 Ma. This pattern is suggested to reflect deep water circulation changes that were triggered by cooling of the Southern Ocean. This first cooling period prior to the CMBE that is also documented by a slight shift toward less radiogenic Nd isotope signatures has not been resolved in previous low-resolution records.

[42] 4. Relatively fast bottom water cooling by up to ~3°C and a parallel marked shift to less radiogenic Nd isotope signatures between 72.5 and 69.5 Ma suggest a substantial change in deep-ocean circulation with significant advection of cooler deep waters with Southern Ocean provenance into the tropical Pacific. The 3.5 million-year-long cooling period in the early Maastrichtian is related to the initial CMBE-$\delta^{13}C$ fall and the subsequent $\delta^{13}C$ rise toward the MME, both representing tectonically forced long-term changes in the global carbon cycle.

[43] 5. After 69.5 Ma, a shift toward more radiogenic Nd isotope values and parallel bottom water warming indicate the return to previous condition with a small contribution of SCW in the late Maastrichtian.

[44] Our high-resolution data show systematic changes in ocean circulation during the Campanian to Maastrichtian that are paralleled by global warming and cooling phases as inferred from benthic foraminiferal stable isotope records. This suggests that the observed variable contributions of SCW within the tropical Pacific were the expression of an enhanced respectively weakened ocean circulation most likely related to the rate of deep water production in the Southern Ocean.

[45] **Acknowledgments.** We are grateful to Claudia Teschner, Roland Stumpf, and Anne Osborne from GEOMAR, Kiel, for providing laboratory know-how and technical support. Jens Fiebig and Sven Hofmann, Stable Isotope Lab Frankfurt, are thanked for stable isotope analyses and Eike Inacker, Maximilian Trapp, Sabrina Morbitzer, Julia Hoffmann, and Oliver Knebel (all Frankfurt) for laboratory assistance. This research used samples provided by the Ocean Drilling Program (ODP). ODP was sponsored by the US National Science Foundation (NSF) and participating countries under the management of Joint Oceanographic Institution (JOI), Inc. We also want to acknowledge the insightful comments of two anonymous reviewers that significantly improved the manuscript. Funding for this project was provided by the German Research Foundation (DFG) (SPP 527 grants VO 687/10-1, 10-2 to S.V. and FR 1198/7-1, -10-2 to M.F., and Emmy Noether research grant Fr 2544/2-1 to O.F.).

References

Arsouze, T., J.-C. Dutay, F. Lacan, and C. Jeandel (2009), Reconstructing the Nd oceanic cycle using a coupled dynamical–biogeochemical model, *Biogeosci. Discuss.*, *6*, 5549–5588.

Arthur, M. A., and A. G. Fischer (1977), Upper Cretaceous–Paleocene magnetic stratigraphy at Gubbio, Italy I. Lithostratigraphy and sedimentology, *Geol. Soc. Am. Bull.*, *88*, 367–371.

Barrat, J. A., F. Keller, and J. Amossé (1996), Determination of rare earth elements in sixteen silicate reference samples by ICP-MS after Tm addition and ion exchange separation, *Geostand. Newsl.*, *20*, 133–139.

Barrera, E. (1994), Global environmental changes preceding the Cretaceous-Tertiary boundary: Early–Late Maastrichtian transition, *Geology*, *22*, 877–880.

Barrera, E., and S. M. Savin (1999), Evolution of late Campanian-Maastrichtian marine climates and oceans, in *Evolution of the Cretaceous Ocean-Climate System*, vol. 332, edited by E. J. Barrera and C. C. Johnson, pp. 245–282, Special Paper Geological Society of America, Boulder, Colo.

Barrera, E., S. M. Savin, E. Thomas, and C. E. Jones (1997), Evidence for thermohaline-circulation reversals controlled by sea-level change in the latest Cretaceous, *Geology*, *25*, 715–718.

Bayon, G., C. R. German, R. M. Boella, J. A. Milton, R. N. Taylor, and R. W. Nesbitt (2002), An improved method for extracting marine sediment fractions and its application to Sr and Nd isotopic analysis, *Chem. Geol.*, *187*, 179–199.

Bralower, T. J., et al. (2002a), Site 1210B Shatsky Rise, ODP Leg 198, *Proc. Ocean Drill. Program: Initial Rep.*, *198*, 1–89.

Bralower, T. J., et al. (2002b), Leg 198 summary, *Proc. Ocean Drill. Program: Initial Rep.*, *198*, 148.

Coffin, M. F., M. S. Pringle, R. A. Duncan, T. P. Gladczenko, M. Storey, R. D. Müller, and L. A. Gahagan (2002), Kerguelen hotspot magma output since 130 Ma, *J. Petrol.*, *43*, 1121–1139.

Cohen, A. S., R. K. O'Nions, R. Siegenthaler, and W. L. Griffin (1988), Chronology of the pressure-temperature history recorded by a granulite terrain, *Contrib.Mineral. Petrol.*, *98*, 303–311.

DePaolo, D. J., and G. J. Wasserburg (1976), Nd isotopic variations and petrogenetic models, *Geophys. Res. Lett.*, *3*, 249–252.

D'Hondt, S., and M. A. Arthur (2002), Deep water in the late Maastrichtian ocean, *Paleoceanography*, *17*(1), 1008, doi:10.1029/1999PA000486.

D'Hondt, S., and M. Lindinger (1994), A stable isotopic record of the Maastrichtian ocean-climate system: South Atlantic DSDP site 528, *Palaeogeogr. Palaeoclimatol. Palaeoecol.*, *112*, 363–378.

Forster, A., S. Schouten, M. Baas, and J. S. S. Damste (2007), Mid-Cretaceous (Albian-Santonian) sea surface temperature record of the tropical Atlantic Ocean, *Geology*, *35*, 919–922.

Frank, T. D., and M. A. Arthur (1999), Tectonic forcings of Maastrichtian ocean-climate evolution, *Paleoceanography*, *14*, 103–117.

Frank, M., N. Whiteley, S. Kasten, J. R. Hein, and K. O'Nions (2002), North Atlantic deep water export to the Southern Ocean over the past 14 Myr: Evidence from Nd and Pb isotopes in ferromanganese crusts, *Paleoceanography*, *17*(2), 1022, doi:10.1029/2000PA000606.

Frank, T. D., D. J. Thomas, R. M. Leckie, M. A. Arthur, P. R. Bown, K. Jones, and J. A. Lees (2005), The Maastrichtian record from Shatsky Rise (northwest Pacific): A tropical perspective on global ecological and oceanographic changes, *Paleoceanography*, *20*, PA1008, doi:10.1029/2004PA001052.

Frey, F. A., et al. (2000), Origin and evolution of a submarine large igneous province: The Kerguelen Plateau and Broken Ridge, southern Indian Ocean, *Earth Planet. Sci. Lett.*, *176*, 73–89.

Friedrich, O., J. O. Herrle, P. Kößler, and C. Hemleben (2004), Early Maastrichtian stable isotopes: Changing deep water sources in the North Atlantic?, *Palaeogeogr. Palaeoclimatol. Palaeoecol.*, *211*, 171–184.

Friedrich, O., J. O. Herrle, P. A. Wilson, M. J. Cooper, J. Erbacher, and C. Hemleben (2009), Early Maastrichtian carbon cycle perturbation and cooling event: Implications from the South Atlantic Ocean, *Paleoceanography*, *24*, PA2211, doi:10.1029/2008PA001654.

Friedrich, O., R. D. Norris, and J. Erbacher (2012), Evolution of middle to Late Cretaceous oceans—A 55 m.y. record of Earth's temperature and carbon cycle, *Geology*, *40*, 107–110.

Gardin, S., B. Galbrun, N. Thibault, R. Coccioni, and I. Premoli Silva (2012), Bio-magnetochronology for the upper Campanian-Maastrichtian from the Gubbio area, Italy: New results from the Contessa Highway and Bottaccione sections, *Newsl. Stratigr.*, *45*(1), 75–103.

Goldstein, S. L., and S. H. Hemming (2003), Long-lived isotopic tracers in oceanography, paleoceanography, and ice sheet dynamics, in *Treatise on Geochemistry*, vol. 17, edited by H. Elderfield, pp. 453–489, Elsevier, New York.

Goldstein, S. J., and S. B. Jacobsen (1987), Nd and Sr isotopic systematics of river water suspended material: Implications for crustal evolution, *Earth Planet. Sci. Lett.*, *87*, 249–265.

Grasse, P., T. Stichel, R. Stumpf, L. Stramma, and M. Frank (2012), The distribution of neodymium isotopes and concentrations in the eastern equatorial Pacific: Water mass advection versus particle exchange, *Earth Planet. Sci. Lett.*, *353-354*, 198–207.

Gutjahr, M., M. Frank, C. H. Stirling, V. Klemm, T. van de Flierdt, and A. N. Halliday (2007), Reliable extraction of a deepwater trace metal isotope signal from Fe–Mn oxyhydroxide coatings of marine sediments, *Chem. Geol.*, *242*, 351–370.

Hague, A. M., D. J. Thomas, M. Huber, R. Korty, S. C. Woodard, and L. B. Jones (2012), Convection of North Pacific deep water during the early Cenozoic, *Geology*, *40*, 527–530.

Haq, B., J. Hardenbol, and P. R. Vail (1987), Chronology of fluctuating sea levels since the Triassic, *Science*, *235*, 1156–1167.

Hay, W. W., R. M. DeConto, C. N. Wold, K. M. Wilson, S. Voigt, M. Schulz, A. Rossby-Wold, W.-C. Dullo, A. B. Ronov, and A. Balukhovsky (1999), Alternative global Cretaceous paleogeography, in *Evolution of the Cretaceous Ocean-Climate System*, vol. 332, edited by E. Barrera and C. C. Johnson, pp. 1–47, Special Paper Geological Society of America, Boulder.

Horikawa, K., E. E. Martin, Y. Asahara, and T. Sagawa (2011), Limits on conservative behavior of Nd isotopes in seawater assessed from analysis of fish teeth from Pacific core tops, *Earth Planet. Sci. Lett.*, *310*, 119–130.

Horwitz, P. E., R. Chiarizia, and M. L. Dietz (1992), A novel strontium-selective extraction chromatographic resin*, *Solvent Extr. Ion Exch.*, *10*, 313–336.

Huber, B. T., R. D. Norris, and K. G. MacLeod (2002), Deep-sea paleotemperature record of extreme warmth during the Cretaceous, *Geology*, *30*, 123–126.

Jacobsen, S. B., and G. J. Wasserburg (1980), Sm-Nd isotopic evolution of chondrites, *Earth Planet. Sci. Lett.*, *50*, 139–155.

Jarvis, I., A. Mabrouk, R. T. J. Moody, and S. de Cabrera (2002), Late Cretaceous (Campanian) carbon isotope events, sea-level change and correlation of the Tethyan and Boreal realms, *Palaeogeogr. Palaeoclimatol. Palaeoecol.*, *188*, 215–248.

Jarvis, I., A. S. Gale, H. C. Jenkyns, and M. A. Pearce (2006), Secular variation in Late Cretaceous carbon isotopes: A new $\delta^{13}C$ carbonate reference curve for the Cenomanian–Campanian (99.6–70.6 Ma), *Geol. Mag.*, *143*, 561–608.

Jeandel, C., T. Arsouze, F. Lacan, P. Téchiné, and J.-C. Dutay (2007), Isotopic Nd compositions and concentrations of the lithogenic inputs into the ocean: A compilation, with an emphasis on the margins, *Chem. Geol.*, *239*, 156–164.

Jenkyns, H. C., A. S. Gale, and R. M. Corfield (1994), Carbon-isotope and oxygen-isotope stratigraphy of the English Chalk and Italian Scaglia and its palaeoclimatic significance, *Geol. Mag.*, *131*, 1–34.

Jiménez Berrocoso, Á., K. G. MacLeod, B. T. Huber, J. A. Lees, I. Wendler, P. R. Bown, A. K. Mweneinda, C. Isaza Londoño, and J. M. Singano (2010), Lithostratigraphy, biostratigraphy and chemostratigraphy of Upper Cretaceous sediments from southern Tanzania: Tanzania drilling project sites 21-26, *J. Afr. Earth Sci.*, *57*, 47–69.

Jiménez Berrocoso, Á., et al. (2012), Lithostratigraphy, biostratigraphy and chemostratigraphy of Upper Cretaceous and Paleogene sediments from southern Tanzania: Tanzania Drilling Project Sites 27–35, *J. Afr. Earth Sci.*, *70*, 36–57.

Jung, C., S. Voigt, and O. Friedrich (2012), High-resolution carbon-isotope stratigraphy across the Campanian–Maastrichtian boundary at Shatsky Rise (tropical Pacific), *Cretaceous Res.*, *37*, 177–185.

Kaiho, K. (1999), Evolution in the test size of deep-sea benthic foraminifera during the past 120 m.y, *Mar. Micropaleontol.*, *37*, 53–65.

Kamenkovich, I., J. Marotzke, and P. H. Stone (2000), Factors affecting heat transport in an ocean general circulation model, *J. Phys. Oceanogr.*, *30*, 175–194.

Koch, M. C., and O. Friedrich (2012), Campanian-Maastrichtian intermediate- to deep-water changes in the high latitudes: Benthic foraminiferal evidence, *Paleoceanography*, *27*, PA2209, doi:10.1029/2011PA002259.

Kuiper, K. F., A. Deino, F. J. Hilgen, W. Krijgsman, P. R. Renne, and J. R. Wijbrans (2008), Synchronizing rock clocks of earth history, *Science*, *320*, 500–504.

Lacan, F., and C. Jeandel (2005), Neodymium isotopes as a new tool for quantifying exchange fluxes at the continent–ocean interface, *Earth Planet. Sci. Lett.*, *232*, 245–257.

Larson, R. L., and W. C. Pitman (1972), World-wide correlation of Mesozoic magnetic anomalies, and its implications, *Geol. Soc. Am. Bull.*, *83*, 3645–3662.

Larson, R. L., M. B. Steiner, E. Erba, and Y. Lancelot (1992), *Proceedings of the Ocean Drilling Program, Scientific Results*, vol. 129, edited by R. L. Larson et al., pp. 615–631, Ocean Drilling Program, College Station, TX.

Le Fèvre, B., and C. Pin (2005), A straightforward separation scheme for concomitant Lu-Hf and Sm-Nd isotope ratio and isotope dilution analysis, *Anal. Chim. Acta*, *543*, 209–221.

Le Houedec, S., L. Meynadier, J.-P. Cogné, C. J. Allègre, and A. T. Gourlan (2012), Oceanwide imprint of large tectonic and oceanic events on

seawater Nd isotope composition in the Indian Ocean from 90 to 40 Ma, *Geochem. Geophys. Geosyst.*, *13*, Q06008, doi:10.1029/2011GC003963.

Lees, J. A., and P. R. Bown (2005), Upper Cretaceous calcareous nannofossil biostratigraphy, ODP Leg 198 (Shatsky Rise, northwest Pacific Ocean), in *Proceedings of the Ocean Drilling Program, Scientific Results*, edited by T. J. Bralower, I. Premoli Silva, and M. J. Malone, pp. 1–60, Ocean Drilling Program, College Station, TX.

Li, L., and G. Keller (1998), Maastrichtian climate, productivity and fauna1 turnovers in planktic foraminifera in South Atlantic DSDP sites 525A and 21, *Mar. Micropaleontol.*, *33*, 55–86.

Li, L., and G. Keller (1999), Variability in Late Cretaceous climate and deep waters: Evidence from stable isotopes, *Mar. Geol.*, *161*, 171–190.

Li, L. Q., G. Keller, T. Adatte, and W. Stinnesbeck (2000), Late Cretaceous sea-level changes in Tunisia: A multi-disciplinary approach, *J. Geol. Soc.*, *157*, 447–458.

MacLeod, K. G., B. T. Huber, and P. D. Ward (1996), The biostratigraphy and paleobiogeography of Maastrichtian inoceramids, in *Special Paper, 307: The Cretaceous-Tertiary Event and Other Catastophes in Earth History*, edited by G. Ryder, D. Fastovsky, and S. Gartner, pp. 361–373, Geological Society of America, Boulder.

MacLeod, K. G., E. E. Martin, and S. W. Blair (2008), Nd isotopic excursion across Cretaceous ocean anoxic event 2 (Cenomanian-Turonian) in the tropical North Atlantic, *Geology*, *36*, 811–814.

MacLeod, K. G., C. I. Londono, E. E. Martin, A. J. Berrocoso, and C. Basak (2011), Changes in North Atlantic circulation at the end of the Cretaceous greenhouse interval, *Nat. Geosci.*, *4*, 779–782.

Martin, E. E., S. W. Blair, G. D. Kamenov, H. D. Scher, E. Bourbon, C. Basak, and D. N. Newkirk (2010), Extraction of Nd isotopes from bulk deep sea sediments for paleoceanographic studies on Cenozoic time scales, *Chem. Geol.*, *269*, 414–431.

Martin, E. E., K. G. MacLeod, A. Jiménez Berrocoso, and E. Bourbon (2012), Water mass circulation on Demerara Rise during the Late Cretaceous based on Nd isotopes, *Earth Planet. Sci. Lett.*, *327–328*, 111–120.

McArthur, J. M., R. J. Howarth, and G. A. Shields (2012), Strontium isotope stratigraphy, in *The Geologic Time Scale 2012*, vol. 1, edited by F. M. Gradstein, pp. 127–144, Cambridge Univ. Press, Cambridge.

Miller, K. G., E. Barrera, R. K. Olsson, P. J. Sugarman, and S. M. Savin (1999), Does ice drive early Maastrichtian eustasy?, *Geology*, *27*, 783–786.

Miller, K. G., P. J. Sugarman, J. V. Browning, M. A. Kominz, J. C. Hernández, R. K. Olsson, J. D. Wright, M. D. Feigenson, and W. Van Sickel (2003), Late Cretaceous chronology of large, rapid sea-level changes: Glacioeustasy during the greenhouse world, *Geology*, *31*, 585–588.

Miller, K. G., J. D. Wright, and J. V. Browning (2005), Visions of ice sheets in a greenhouse world, *Mar. Geol.*, *217*, 215–231.

Müller, R. D., M. Sdrolias, C. Gaina, and W. R. Roest (2008a), Age, spreading rates, and spreading asymmetry of the world's ocean crust, *Geochem. Geophys. Geosyst.*, *9*, Q04006, doi:10.1029/2007GC001743.

Müller, R. D., M. Sdrolias, C. Gaina, B. Steinberger, and C. Heine (2008b), Long-term sea-level fluctuations driven by ocean basin dynamics, *Science*, *319*, 1357–1362.

Murphy, D. P., and D. J. Thomas (2012), Cretaceous deep-water formation in the Indian sector of the Southern Ocean, *Paleoceanography*, *27*, PA1211, doi:10.1029/2011PA002198.

Nakanishi, M., K. Tamaki, and K. Kobayashi (1989), Mesozoic magnetic anomaly lineations and seafloor spreading history of the northwestern Pacific, *J. Geophys. Res.*, *94*, 437–462.

Odin, G. S., and M. A. Lamaurelle (2001), The global Campanian-Maastrichtian stage boundary, *Episodes*, *24*, 229–238.

Paull, C. K., S. J. Hills, and H. R. Thierstein (1988), Progressive dissolution of fine carbonate particles in pelagic sediments, *Mar. Geol.*, *81*, 27–40.

Petrizzo, M. R., F. Falzoni, and I. Premoli Silva (2011), Identification of the base of the lower-to-middle Campanian *Globotruncana ventricosa* zone: Comments on reliability and global correlations, *Cretaceous Res.*, *32*, 387–405.

Piotrowski, A. M., A. Galy, J. A. L. Nicholl, N. Roberts, D. J. Wilson, J. A. Clegg, and J. Yu (2012), Reconstructing deglacial North and South Atlantic deep water sourcing using foraminiferal Nd isotopes, *Earth Planet. Sci. Lett.*, *357-358*, 289–297.

Premoli Silva, I., and W. Sliter (1995), Cretaceous planktonic foraminiferal biostratigraphy and evolutionary trends from the Bottaccione section Gubbio, Italy, *Palaeontographia Italica*, *82*, 1–89.

Pucéat, E., C. Lécuyer, and L. Reisberg (2005), Neodymium isotope evolution of NW Tethyan upper ocean waters throughout the Cretaceous, *Earth Planet. Sci. Lett.*, *236*, 705–720.

Robinson, S. A., and D. Vance (2012), Widespread and synchronous change in deep-ocean circulation in the North and South Atlantic during the Late Cretaceous, *Paleoceanography*, *27*, PA1102, doi:10.1029/2011PA002240.

Robinson, S. A., D. P. Murphy, D. Vance, and D. J. Thomas (2010), Formation of "Southern Component Water" in the Late Cretaceous: Evidence from Nd-isotopes, *Geology*, *38*, 871–874.

Roy, M., T. van de Flierdt, S. R. Hemming, and S. L. Goldstein (2007), $^{40}Ar/^{39}Ar$ ages of hornblende grains and bulk Sm/Nd isotopes of circum-Antarctic glacio-marine sediments: Implications for sediment provenance in the southern ocean, *Chem. Geol.*, *244*, 507–519.

Siddall, M., S. Khatiwala, T. van de Flierdt, K. M. Jones, S. L. Goldstein, S. R. Hemming, and R. F. Anderson (2008), Towards explaining the Nd paradox using reversible scavenging in an ocean general circulation model, *Earth Planet. Sci. Lett.*, *274*, 448–461.

Soudry, D., C. R. Glenn, Y. Nathan, I. Segal, and D. VonderHaar (2006), Evolution of Tethyan phosphogenesis along the northern edges of the Arabian-African shield during the Cretaceous-Eocene as deduced from temporal variations of Ca and Nd isotopes and rates of P accumulation, *Earth Sci. Rev.*, *78*, 27–57.

Stumpf, R., M. Frank, J. Schönfeld, and B. A. Haley (2010), Late Quaternary variability of Mediterranean outflow water from radiogenic Nd and Pb isotopes, *Quat. Sci. Rev.*, *29*, 2462–2472.

Tachikawa, K., C. Jeandel, and M. Roy-Barman (1999), A new approach to the Nd residence time in the ocean: The role of atmospheric inputs, *Earth Planet. Sci. Lett.*, *170*, 433–446.

Tanaka, T., et al. (2000), JNdi-1: A neodymium isotopic reference in consistency with LaJolla neodymium, *Chem. Geol.*, *168*, 279–281.

Thibault, N., D. Husson, R. Harlou, S. Gardin, B. Galbrun, E. Huret, and F. Minoletti (2012a), Astronomical calibration of upper Campanian–Maastrichtian carbon isotope events and calcareous plankton biostratigraphy in the Indian Ocean (ODP Hole 762C): Implication for the age of the Campanian–Maastrichtian boundary, *Palaeogeogr. Palaeoclimatol. Palaeoecol.*, *337-338*, 52–71.

Thibault, N., R. Harlou, N. Schovsbo, P. Schioler, B. W. Lauridsen, E. Sheldon, L. Stemmerik, and F. Surlyk (2012b), Upper Campanian–Maastrichtian carbon-isotope stratigraphy of the Danish Basin: Calibration with calcareous nannofossil and dinoflagellate events in the Boreal Realm, *Cretaceous Res.*, *33*, 72–90.

Thomas, D. J. (2004), Evidence for deep-water production in the North Pacific Ocean during the early Cenozoic warm interval, *Nature*, *430*, 65–68.

Thomas, D. J., T. J. Bralower, and C. E. Jones (2003), Neodymium isotopic reconstruction of late Paleocene-early Eocene thermohaline circulation, *Earth Planet. Sci. Lett.*, *209*, 309–322.

Voigt, S., O. Friedrich, R. D. Norris, and J. Schönfeld (2010), Campanian–Maastrichtian carbon isotope stratigraphy: Shelf-ocean correlation between the European shelf sea and the tropical Pacific Ocean, *Newsl. Stratigr.*, *44*, 57–72.

Voigt, S., A. S. Gale, C. Jung, and H. C. Jenkyns (2012), Global correlation of Upper Campanian-Maastrichtian successions using carbon-isotope stratigraphy: Development of a new Maastrichtian timescale, *Newsl. Stratigr.*, *45*, 25–53.

Voigt, S., C. Jung, O. Friedrich, M. Frank, C. Teschner, and J. Hoffmann (2013), Tectonically restricted deep-ocean circulation at the end of the Cretaceous greenhouse, *Earth Planet. Sci. Lett.*, *369-370*, 169–177.

Wilson, D. J., A. M. Piotrowski, A. Galy, and J. A. Clegg (2013), Reactivity of neodymium carriers in deep sea sediments: Implications for boundary exchange and paleoceanography, *Geochim. Cosmochim. Acta*, *109*, 197–221.

Zachos, J., M. Pagani, L. Sloan, E. Thomas, and K. Billups (2001), Trends, rhythms, and aberrations in global climate 65 Ma to present, *Science*, *292*, 686–693.